Experimental Analysis of Solar Assisted Refrigerating Electric Vehicle

Surender Kumar, Rabinder Singh Bharj

Abstract*: Most refrigerating systems are driven by an internal combustion engine that increased the conventional vehicle's oil consumption and tailpipe emissions. The solar-assisted refrigerating electric vehicle (SAREV) system powered by a hybrid energy mode has been designed. The hybrid energy (solar + grid) was stored in the battery bank to complete this vehicle's necessary functions. The PV panels are prominently incorporated into this vehicle rooftop to charge the battery bank. In this study, the integrated system was driven by a hybrid energy mode that reducing the wastage and deterioration during temporary storage and transportation in different areas. The performance of the integrated system was tested under different operating conditions. The effect of load variation on maximum speed and travelling distance of vehicle was analyzed. The battery bank charging and discharge performance were studied with and without solar energy. The refrigerator was consuming 116 Wh energy per day to maintain a -12 ^{o}C lower temperature on the no-load condition at the higher thermostat position. The refrigerator was run continuously for 4-6 days on battery bank energy and 7-10 days on the full load condition of hybrid energy. The vehicle was travelling at a maximum of 23 km/h speed on full load condition. The vehicle needed torque 14-16 N-m at the initial phase for each load condition. Torque demand was decreasing with the increasing speed of the vehicle. The full-charged battery bank's initial voltage was 51.04 V, and the cut-off voltage was 46.51 V. The vehicle was covering a distance of 62.4 km with the battery bank alone at full load condition. It was travelling 68.3 km distance with hybrid energy mode. The vehicle's integrated system was the best in maintaining battery performance, power contribution capability, and drive range enhancement.

Keywords: Photovoltaic (PV) module, Maximum power point tracking, Refrigerated electric vehicle (REV) performance, Energy consumption.

I. INTRODUCTION

Energy sources are the key pillars for the survival of human beings in the current society. These energy sources play a significant role in developing modern society and various industrial sectors in developing countries [1]. The demand for electric vehicles (EVs) increases with augmented restrictions on greenhouse gas (GHG) emissions. Today, SAREV is considered a vital pathway to meet future environmental impact requirements [2]. Electric vehicles (EVs) are one of the primary modes of passenger and goods transportation in congested areas of the megacity. Conventional vehicles impart a vital role in the social and economic development of a country. However, these vehicles are consuming a higher amount of fossil fuels, leading the GHG emissions. Different types of conventional vehicles are used in the megacity, which poses severe pollution issues, higher energy consumption, traffic congestion, high noise, and road accidents. The harmful GHG emissions are the leading cause of global warming and severe health problems such as cardiac events, visibility, difficulty breathing, asthma, or even death in humans [3]. In most Indian megacities, the tailpipe emissions of conventional vehicles are the leading cause of atmospheric particles. The tailpipe emissions can be reduced in megacities using the EVs in place of internal combustion engines (ICE) vehicles. The maximum street vendors and customers are at the risk of health deterioration due to vehicular emission. The Street Vendors Act was enacted in 2014 in India, but this act does not cover any issue related to their health perspectives [4]. The health risk of street vendors can be reduced by wearing an N-95 nose mask and decreasing vehicular tailpipe emissions. The development of carbon-free megacities is one of the prime goals of many governments all over the world. This target can be achieved globally by gradually reducing fossil fuels and promoting solar energy in different sectors [5]. Therefore, the vehicle manufacturing industries are moving toward developing the latest EVs using the latest technologies and materials. The transportation sector contributes alone to about 30% of total world GHG emissions that play a significant role in the built environment in urban areas [6]. In recent years, the solar panels are mounting on EV's rooftop for charging the battery bank, which minimizes the grid dependency and maximizes green energy technologies. Solar-powered charging stations connect to the electric grid that ensures the profits to the entrepreneurs of charging stations [7-9]. The average sun hours and sunny days in the last five years for Jalandhar city (Punjab) are shown in figure 1 [10]. The vehicle PV roof receives 58% of the available solar radiation in real-world conditions [11]. Refrigerated road transportation (RRT) is recognized to consume higher energy in the current cold chain. The refrigerated vehicles consume 20-30% extra fuel compared to the standard delivery ICE based vehicles. The carbon emission of different traveled road vehicles per kilometer is shown in figure 2. The fresh food demand is continuously increasing due to the increasing worldwide population. The refrigerated vehicles (RVs) are essential for maintaining the refrigerated space's lower temperature at the required level.

Manuscript received on January 18, 2021.
Revised Manuscript received on February 03, 2021.
Manuscript published on January 30, 2021.
* Correspondence Author
Surender Kumar, Research Scholar, Mechanical Engineering Department, National Institute of Technology, Jalandhar (Punjab), India.
Dr. R.S. Bharj*, Associate Professor, Mechanical Engineering Department, National Institute of Technology, Jalandhar (Punjab), India.

The ICE-based RVs are confronting some restrictions that available in the current market [12]. These RVs are suitable for a wide range of deliveries from one city to another city. For intercity goods home deliveries with small quantities, the RVs are not much energy efficient and economical. Therefore, energy-efficient refrigerated vehicles are required in the refrigerated road transportation system [13]. The refrigerated electric vehicles (REVs) having 100-250 kgs storage capacity are suitable for intercity deliveries in congested city zones. These vehicles are considered a suitable alternative for traditional RVs due to their energy-savings and GHG emission reduction. Adopting the SAREV is the best alternative compared to conventional refrigerated vehicles concerning their life-cycle emissions, costs, and externalities [14-16]. This study attempts to fill this research gap by looking at alternatives in cold chain transportation that support efforts to increase sustainability in urban home deliveries. The vehicle used in this analysis is the best alternative in cold chain vehicle types. The energy consumption test of this vehicle is carrying out under varying operating conditions in this study. Additionally, this study focuses on the cost analysis of this vehicle. This paper focused on SAREV that can reduce energy consumption by adjusting the vehicle speed and thermostat position. The paper is organized as follows: Section II of the paper provides the literature related study on the REVs. The design and longitudinal models of vehicle are presenting in section III. The description of this vehicle is presenting in section IV. The performance of this vehicle is furnishing in section V.

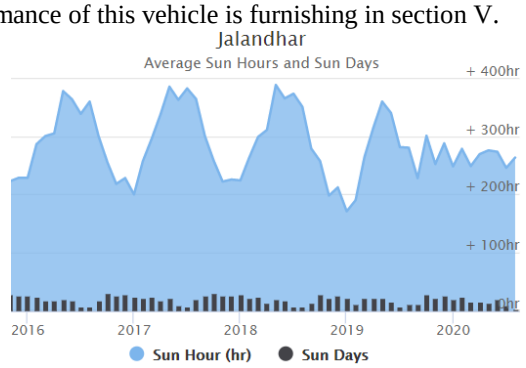

Fig. 1.The average availability of sun hours and sunny days in the last five years for Jalandhar city (Punjab) [11].

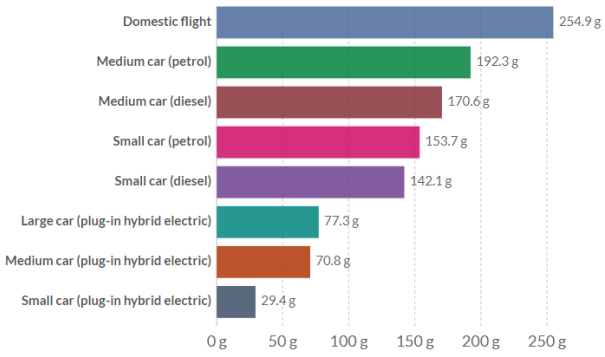

Fig. 2.Carbon emission by different type of road vehicles per kilometere [14].

II. LITERATURE REVIEW

Numerous research articles have been published lately in the literature that has addressed the future of RRT vehicles. Some of these studies focused on analyzing and comparing alternative cooling technologies used in load-carrying vehicles. Few of them from these studies were mainly focusing on their environmental and cost impacts (see table-I). The conventional road refrigerated vehicles were lower energy efficiency and not much cost optimizer. The maximum refrigeration systems were driven by an internal combustion engine that consumed 20-30% more fuel than an unrefrigerated conventional vehicle. The freight transport system was consuming nearly a quarter of all the petroleum worldwide, which produced more than 10% of GHG emissions from fossil fuels. The refrigerated road vehicles (IC trucks & electric trucks) were not suitable for small order delivery in the congested city zone. For quality expectations in goods home delivery, the road transport refrigeration system was demanding higher energy-efficient vehicles. The proposed vehicle can complete all these demands. Therefore, the present research work focuses on the performance analysis of the SAREV. However, limited information about the SAREV has been found in past literature studies.

III. ENERGY CONSUMPTION AND THE DRIVING RENGE OF VEHICLE

This vehicle's drive range depends on several factors such as vehicle mass and shape, available energy (storage energy and solar energy), internal resistance, etc. This driving range is measured with the total energy stored in the battery bank. Figure 3 shows that the forces and movements act on the SAREV in the longitudinal direction when the road has a positive slope (α). The external resistive driving forces acting on this vehicle in the longitudinal direction are named air drag force ((F_{drag}), rolling resistance (F_{roll}), and gradient resistance (F_{grad}). This vehicle is transmitted torque through the electric motor shaft, which used battery power. Tractive effort ($F_{tractive}$) is required to move this vehicle in the longitudinal direction [28]. The mathematical expression (Newton Second Laws of motion) between forces and acceleration in the longitudinal direction (X-direction) for the vehicle is shown by equation (1).

$$F_{tractive} = \lambda M \frac{dV_x}{dt} + \sum F_{resistive} \quad (1)$$

$F_{tractive}$ is the total tractive effort acting on the wheel of this vehicle in the x-direction, M is the total mass of this vehicle, dV_X/dt is torque required to move this vehicle, or electric propulsion to overtake the resistive forces. The resistive forces acting on this vehicle in the x-direction are presented in equation (2).

$$\sum F_{resistive} = \underbrace{Mg\sin\alpha}_{grade} + \underbrace{Mg\mu_r\cos\alpha}_{roll} + \frac{1}{2}\underbrace{\rho A_f C_D V_X^2}_{drag} \quad (2)$$

α is the road slope angle, g is the gravitational constant, μ_r is the rolling coefficient of friction (between the contact point of tire and road), ρ is the air density, A_f is

Table- I: Review for RRT vehicles

Reference	Year	Refrigerated vehicle type	Method & experimental parameters	Location	Short description of the article
[17]	2009	VCS refrigerated engine vehicle	• Mechanical VCR system; • Energy consumption by the refrigerating unit; • Environmental impacts.	United Kingdom	Refrigerated diesel vehicles consumed 40% more fuel as compared to conventional vehicles
[18]	2010	Refrigerated truck	• Nonlinear refrigerated transport system model; • Compressor speed with time; • Refrigerating unit temperature.	USA	During transportation, the model controlled the compressor's on-off in the VCR system and maintained a lower desire temperature by consuming less energy inside cargo space.
[19]	2014	Refrigerated van	• 2D FEM model; • Heat transfer coefficient and temperature of multilayer; • Heat flux densities for insulating walls.	France	The reduction of heat transfer and energy consumption was analyzed by increasing the multilayer panel thickness by 20-36% during the daytime.
[20]	2015	Refrigerated truck	• The CFD model; • Temperature and velocity profile by adjusting the time; • Experimental heat flow rate.	France	The velocity profile variation (-20 to 40 °C) was analyzed with full aperture, 1/3 aperture, and 2/3 aperture.
[21]	2017	Cryogenic transport with diesel engines	• Cryogenic transport refrigeration system; • Speed of vehicle in the urban and rural area; • Ambient temperature change with time; • The temperature inside refrigerated space; • Different load distribution on engine load.	United Kingdom	The emission of diesel cryogenic was 66% lower as compared to the VCS-diesel system.
[22]	2017	PU-PCM based refrigerated vehicle	• The dynamic 1D model was solved with the FEM; • Heat flux densities and temperatures measured at different composite walls; • Specific heat capacity of pure PCM, pure PU foam, and composites (PU-PCM).	France	The refrigerated vehicles used a composite layer of PU-PCM foam that finds high energy storage capacities.
[23]	2018	Refrigerated transport	• Multi-period optimization model; • Temperatures and power consumption of vehicle; • Search the best route for urban deliveries.	Italy	The best route was highlighted for food deliveries that control fuel consumption and refrigeration energy. The optimal direction was best (1-3-4-2-1) in terms of fuel consumption.
[24]	2019	Refrigerated truck	• The dynamic model for vehicle insulated box; • Inside and outside wall temperatures; • Solar radiation and convective heat transfer rate; • Power consumed by the cooling unit.	Italy	The vehicle cabin thermal capacity was 47% higher, and the thermal resistance was 23% lower than the stratigraphy values.
[25]	2019	VCS-refrigerated vehicle	• The CFD shear stress transport calculation model used; • Temperatures inside the cooling chamber; • Airflow lines inside the refrigerated vehicle.	Ecuador	The air outlet system's temperature distribution was similar to the experimental curve with an average temperature variation of 0.43 °C. The average temperature variation was 0.34 °C for the vehicle floor, and the truck door average temperature variation was 0.07 °C.
[26]	2019	Refrigerated trailer	• Numerical method; • Temperatures inside the trailer; • Heat transfer coefficients of stored products.	France	The ham part's h_c values were higher compared to loin and shoulder parts everywhere in the trailer. The low airflow was recorded because two carcasses located side-by-side are in contact on the rind side with the ham part. The h_c (5–7 W/m^2. k) was almost stable in the trailer.
[27]	2020	LNG-fueled refrigerated vehicles	• TRNSYS software; • LNG flow rate and ambient temperature; • The radiant roof temperature and air temperature.	China	The vehicle was operated at an economical speed; the refrigerating system's cooling capacity was 1.2 kW.

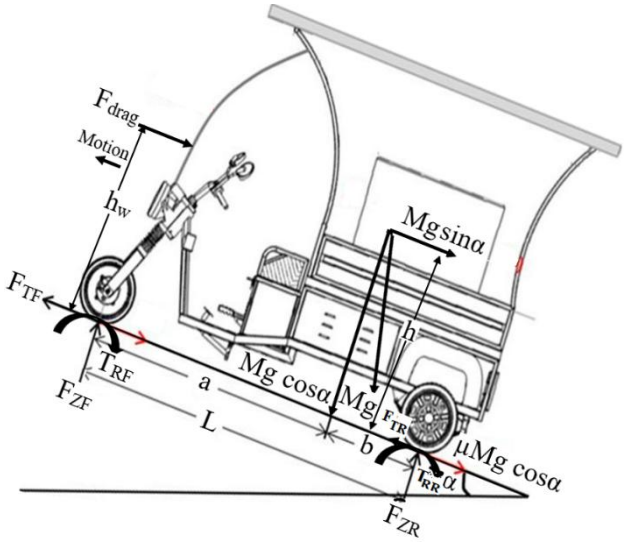

Fig. 3.Force acting on the model of the SAREV.

Fig. 4.Table- II: Mechanical designed parameters of vehicle

Design parameters	Design value	SI unit
The air density (ρ)	1.220	kg/m^3
The drag coefficient (C_D)	0.333	-
The mass factor of rotation (λ)	1.000	-
The rolling friction coefficient (μ_r)	0.015	-
The front area of the three-wheeled vehicle (A_f)	1.780	m^2
The maximum speed of this vehicle (V_x)	29.000	km/h
The overall efficiency of the drivetrain (η_m)	0.900	-
The estimated weight of the vehicle (M)	500.0	kg
Wheel diameter of this vehicle (d_w)	0.508	m
The wheelbase of this vehicle (L)	2.200	m
Distance between vehicle C.G. and front axle (a)	1.100	m
Distance between vehicle C.G. and rear axle (b)	1.3	m

the front area of this vehicle, the C_D is the air coefficient of drag and V_X is the longitudinal velocity of this vehicle in the longitudinal direction. The tractive effort required for the vehicle is presented in equation (3).

$$F_{tractive} = \lambda M \frac{dV_X}{dt} + \underbrace{Mg \sin\alpha}_{grade} + \underbrace{Mg\mu_r \cos\alpha}_{roll} + \frac{1}{2}\underbrace{\rho A_f C_D V_X^2}_{drag} \quad (3)$$

The normal dynamic load acting in the vertical direction on the front axle is given in equations (4) and (5).

$$F_{ZF} = Mgb\cos\alpha - (T_{RF} + T_{RR} + F_{drag}h_w + Mgh\sin\alpha + \lambda hMdV_x / dt)$$

(4) Taking, $h_w \approx h$

$$F_{ZF} = \frac{Mgb\cos\alpha}{L} - \frac{1}{L}(T_{RF} + T_{RR} + F_{drag}h_w + Mgh\sin\alpha + \lambda hMdV_x / dt)$$

(5) The rolling resistance moments acting between wheel and ground is shown in equation (6). It is the product of rolling resistant force and radius of the tire.

$$T_{RF} + T_{RR} = \mu Mgr_w \cos\alpha \quad (6)$$

M_g is the total weight acting at the center of the wheel, and r_w is the wheel radius. The normal load is acting in the front axle (calculated by Eq. 7) and in the vertical direction on the rear axle (calculated by Eq. 8).

$$F_{ZF} = \frac{Mgb\cos\alpha}{L} - \frac{h}{L}\left(F_{tractive} - \mu_r Mg\cos\alpha\left(1 - \frac{r_W}{h}\right)\right) \quad (7)$$

$$F_{ZR} = \frac{Mgb\cos\alpha}{L} - \frac{h}{L}\left(F_{tractive} - \mu_r Mg\cos\alpha\left(1 - \frac{r_W}{h}\right)\right) \quad (8)$$

The required tractive torque acting on this vehicle wheel comes from the electric propulsion system (motor power) is shown in equation (9).

$$T_{tractive} = \left(\lambda M \frac{dV_X}{dt} + \underbrace{Mg\sin\alpha}_{grade} + \underbrace{Mg\mu_r\cos\alpha}_{roll} + \frac{1}{2}\underbrace{\rho A_f C_D V_X^2}_{drag}\right) r_w \quad (9)$$

$$T_{tractive} = T_{demand} = \left(\lambda M \frac{dV_X}{dt} + \underbrace{Mg\sin\alpha}_{grade} + \underbrace{Mg\mu_r\cos\alpha}_{roll} + \frac{1}{2}\underbrace{\rho A_f C_D V_X^2}_{drag}\right) r_w \times \frac{1}{G_r} \quad (10)$$

Torque demand (T_{demand}) depends on the wheel radius (r_w) and gear ratio (G_r) of this vehicle. The torque helps run the vehicle at the required acceleration provided by the BLDC motor, as shown in equation (10).

$$P_{demand} = T_{demand} \times \frac{S_v}{r_w} \times \omega_w \times G_r \quad (11)$$

The torque limit for the motor is determined from the motor datasheet. The power demand (P_{demand}) of the BLDC motor can be calculated from the linear vehicle speed, as shown in equation (11). Due to rotational friction of the motor, the mechanical spin losses are considered negligible. In this approach, the average motor efficiency is assumed to be 92%. The maximum vehicle speed (S_v) 29 m/s is taken.

$$E_{consumed} = \frac{1}{\Delta t}\int_0^{\Delta t} P_{elect.}(t)dt \quad (12)$$

The energy consumed by the integrated system is shown in equation (12). Energy consumed by this vehicle is integral to electric power required during an amount of time.

$$SOC = \frac{C_{batt.\_kWh} - E_{consumed}}{C_{batt.\_kWh}} \times 100 \quad (13)$$

The state of charge (SOC) for the battery bank depends on the vehicle energy consumption and battery capacity, as shown in equation (13) [28]. The vehicle's mechanical design parameters are shown in Table- II.

A. Carbon emissions from the vehicle

Several numbers of parameters are considered for calculating indirect carbon emissions (SAREV_$C_{emission}$) from the SAREV. These parameters

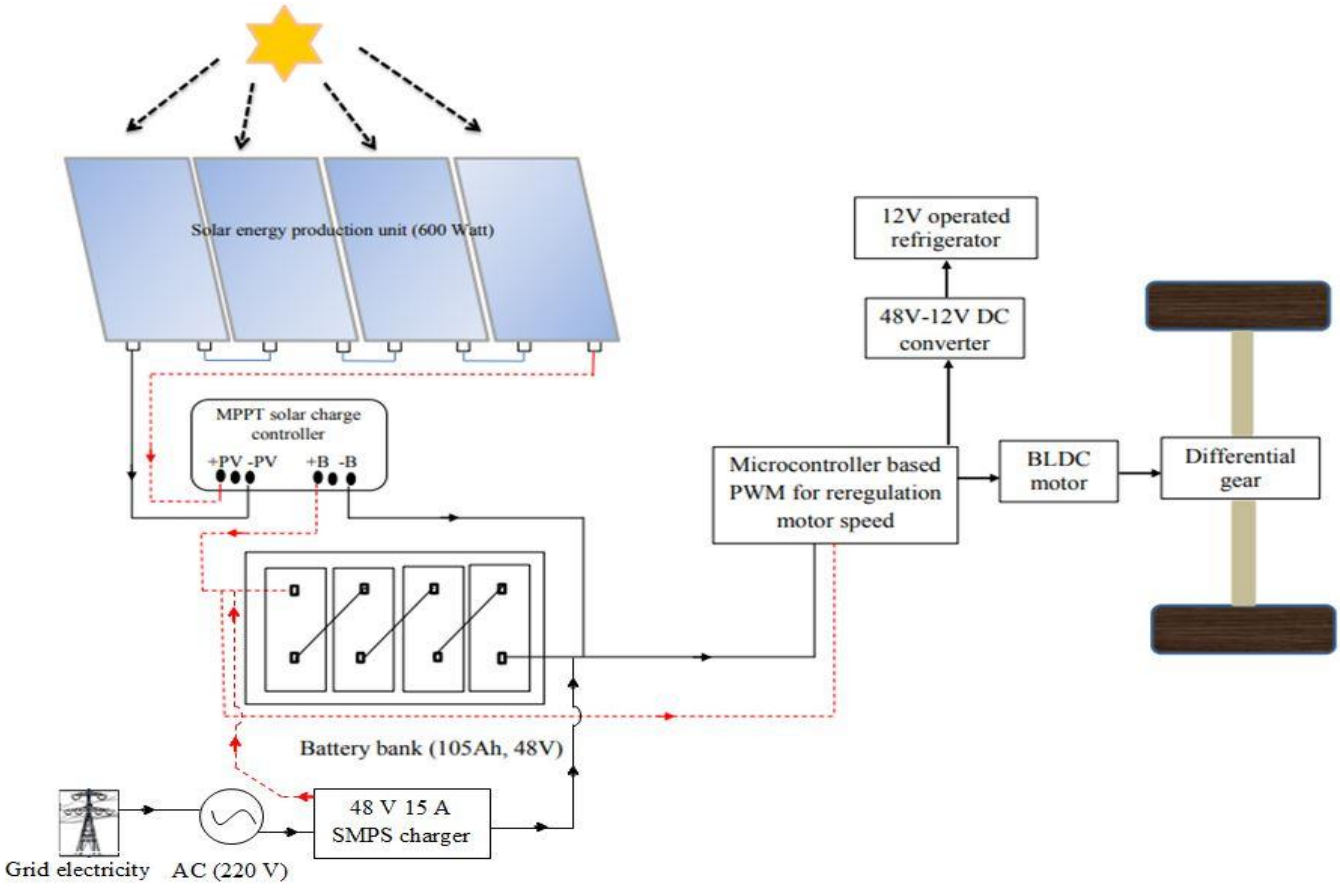

Fig. 4(a). Schematic diagram of the experimental set-up.

$$SAREV\_C_{emission} = SAREV_{power} \times \frac{C_{emission\_electricity}}{1 - L_T} \quad (14)$$

$$C_{emission\_electricity} = \sum_i^n x_i \times w_i = \left[x_{fossil} \times w_{fossil} \right] + \left[x_{renewable} \times w_{renewable} \right] \quad (15)$$

include the power consumption of vehicle ($SAREV_{power}$), carbon emission during electricity generation ($C_{emission\_electricity}$), and transmission losses (L_T) that is around 19% in India. With the use of equations (14 and 15), the vehicle's carbon emission is calculated. The vehicle used two types of energy sources, the first grid energy, and solar energy. The grid energy is generated by fossil fuels, where solar energy is a renewable energy resource. The carbon emissions depend on each energy source's contribution for charging the battery bank of this vehicle, where x_i is the emissions from each energy source, and w_i is the share of a particular energy source in electricity generation [29-30].

IV. DESCRIPTION FOR EXPERIMENTAL SET-UP

The experimental set-up consists of a programmable DC power supply, 12 V DC refrigerator (240 L capacity), solar panels (48 V & 600 W), solar charge controller, lead-acid storage batteries (48 V & 105 Ah), temperature feedback controller, and electromagnetic relay as shown in figure 4(a). The refrigerator is fitted on the backside of this vehicle. The programmable DC power supply controller and refrigerator were purchased from Phocos India Solar Pvt Ltd. However, the solar charge controller and PV panels were purchased from Su-Kam Power Systems LTD. The single PV panel dimension is 1483 mm × 666 mm, with a nominal efficiency of 15% and an output power of 150 W (at 25 ^{o}C and 1000 W/m^2). Four PV panels are installed on the vehicle's roof to charge the battery bank in the daytime. These panels are connected in series. The specification of this vehicle is shown in table 3. The vehicle's refrigerator is driven by a DC compressor K35 DC ROHS Sol-cool. The vehicle's battery bank used four lead-acid batteries that are connected in series. The battery bank rated at 48 V with the capacity of 105 Ah is used for energy storage and used as a power source for running the compressor and BLDC motor. The power generated by solar panels is store in the battery bank via a solar charge controller. For charging the battery bank at night, a 15 A battery charger was purchased from Fujiyama Power Systems PVT. LTD.

In the refrigerator experiments, the cabin walls temperatures are monitored with PT100 thermocouples. The six thermocouples were used for this purpose that purchased from Jiamin instrument CO. LTD. Two digital tachometers (NJK-5002C -Hitsan 4) proximity switch sensors were used to measure motor and vehicle speed. Three digital watt-meters (DC PZEM-051) were used to measure the output current of solar panels, input current of BLDC motor, and DC compressor. These watt-meters were purchased from Unitrend technology CO., LTD. A solar pyranometer (Amprobe solar -100) is used to measure the solar radiation falling on solar panels' surface. A 48-12 V DC converter is used to supply the sufficient low voltage for the refrigerator. The accuracies of the instruments used for the data collection are shown in table 4. The photographic view of this vehicle is shown in figure 4(b).

All experiments were conducted on this vehicle, with the MBH-b Block's location in National Institute of Technology in Jalandhar city of Punjab state in India, between April 5-28th. The following experimental conditions were maintained across this study:

- The DC refrigerator door was kept open for two hours to maintain thermal equilibrium with ambient air before starting each experiment.
- The door of the refrigerator was kept closed during the experiment time.
- The battery bank of the vehicle must be fully charged before starting each the experiment.
- All experiments were performed in sunny days conditions on the same test path.

Table- III: Specification of the components used in vehicle designed

Name of component used (No.)	Parameter name	Specification
Solar panels (4) connected in series	Capacity (W_P)	150 W
	Module volt (V)	12 V
	Width (W) x Height (H) x Thickness (T)	666 mm ×1483 mm × 35 mm
	Open circuit voltage (V_{oc})	21.5 V
	Short circuit current (I_{sc})	8.75 A
	The voltage at maximum power (V_{mp})	18 V
	Current at maximum power (I_{mp})	8.5 A
	Efficency (η_{pv})	15%
MPPT charge controller (1)	System voltage	24/48 auto recognition
	Max charge/ load current	10-45 A
	Efficiency	95%
DC-DC converter (1)	Voltage converting	48 to 12 V DC
Refrigerator (1)	Dimensions of the outer cabinet	1145 mm × 850 mm × 690 mm
	Inner dimensions	900 mm × 673 mm × 440 mm
	Operating voltage	12 V or 24 V DC (normal)
	Temperature range	-16 to +6 ^oC
	Refrigerant used	R-134a (eco-friendly)
	Insulation	Polyurethane (12 cm thick)
	Compressor type	DC compressor (K35 DC Rohs sol-cool)
Lead-acid batteries connected series (4)	Rated output	12V- 105 Ah
	Depth of discharge	80% (First 1600 cycles)
	Overall efficiency	62%
DC motor used (1)	Related output	850 W
	Motor controller output	850 W
Hybrid electric vehicle (two-person seating)	Wheelbase	2105 mm
	L × W × H	2765 mm × 990 mm × 1050 mm
	Load carriage box dimension	1295 mm × 945 mm × 600 mm
	Vehicle weight	460 kg
	Maximum speed	29 km/hour
	Climbing ability	20 % grading
	Rating output	1000 W DC motor
	Brake	Drum type
	Charging time	8 hours
	Tire size	3:0-12
	Charger	48 V & 15 A SMPS charger
	Body material used	High-grade steel

Table- IV: The ranges and accuracies of the main experimental instruments

Parameter	Unit	Range	Accuracy
The solar radiation intensity (G)	W/m^2	0~1999	±1
The ambient temperature (T_a)	^oC	-50~110	±0.15
The refrigerator inside cabin (T_r)	^oC	-50~110	±0.15
The PV panel current (I_{PV})	A	0~10A	±0.005
The PV panel voltage (V_{PV})	V	0~50 V	±0.005
The digital tachometer	rpm	5~9999	±0.2
The wattmeter	V, A	6.5~100V , 0~100A	±0.005

This study starts with a fundamental energy consumption analysis to provide insight into the relationship between

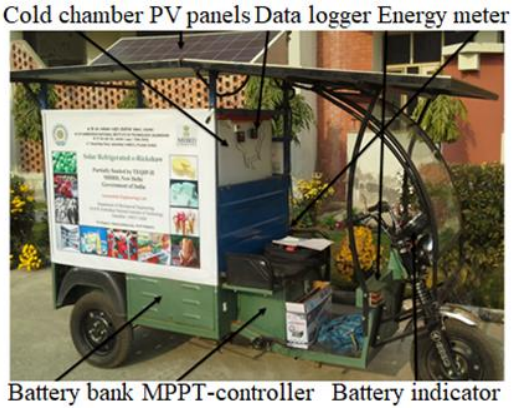

Fig. 4(b). The photographic view of the SAREV.

Fig. 5. Test route used for the SAREV.

energy consumption and vehicle driving parameters. The vehicle driving parameters such as vehicle speed, torque, battery discharge rate, battery current, and voltage were used to calculate this vehicle's instantaneous energy consumption rate. The vehicle's test route is shown in figure 5.

V. RESULT AND DISCUSSION

The experiments were carried out to analyze the performance of this vehicle on typical sunny days. These experiments were divided into three steps. At the first step, the performance of PV panels was tested. In the second step, the refrigerator of this vehicle was tested by varying the thermostat position. In the third step, the performance of this vehicle was tested in different load conditions.

A. The PV Panels Test

The experiment was conducted on a typically sunny day (from 9.00 AM to 5.00 PM). The performance curves of PV panels are shown in figure 6. The output (current, voltage, and power) of the PV panels were recorded. The solar irradiance was recorded 390-1150 W/m^2 on the PV panel surface. The power output was recorded around 300-420 W.

B. Experiments on the DC Refrigerator

All experiments were performed under a no-load condition. These experiments were conducted with the varying position of the thermostat switch from 1 to 7. The energy consumption with temperature variation inside the cabin was recorded. The refrigerator energy consumption is shown in figure 7(a), and temperature variation inside the cabin is shown in figure 7(b). After conducting the refrigerator experiments, the value of energy consumption per day for each thermostat position was recorded as 38 Wh, 63 Wh, 108 Wh, 76 Wh, 58 Wh, 92 Wh, and 116 Wh for the thermostat setting from position 1 to position 7, respectively. The lowest value of temperature was recorded as 2.1 ^{o}C, -1.9 ^{o}C,

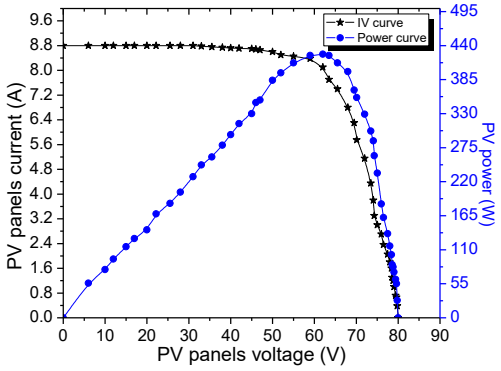

Fig. 6. IV and power curves for four panels used in the vehicle.

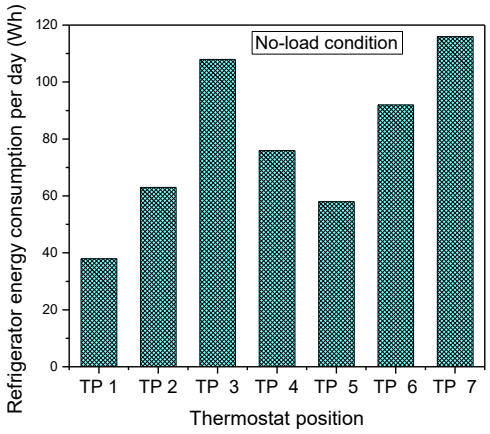

(a)

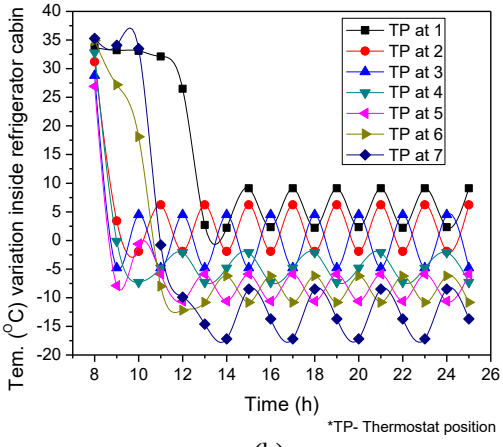

(b)

Fig. 7. Refrigerator (a) energy consumption (b) temperature variation inside cabin.

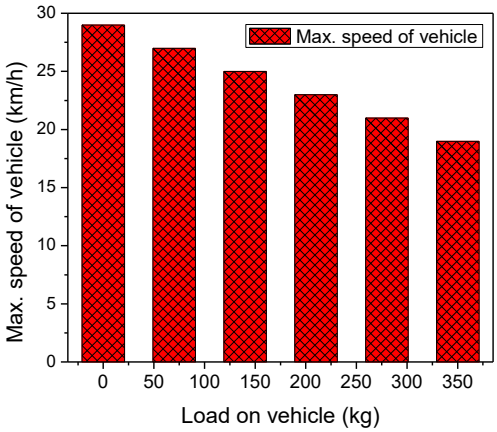

Fig. 8(a). The vehicle maximum speed with load variation.

-6.2 ^{o}C, -7.3 ^{o}C, -10.6 ^{o}C, -12.4 ^{o}C, and -17.7 ^{o}C for the thermostat setting from positions 1 to 7 respectively. At the thermostat position 5, the refrigerator maintains the lower desired temperature inside the cabin within minimum time by consuming less energy.

C. Performance Analysis of Vehicle

The performance analysis of this vehicle is executed to test the charging and discharging features. The battery placed in this vehicle is charged using grid electricity, while the PV panels are used to assist partially charge the battery bank in the day time. The discharging characteristic of the vehicle is analyzed with different load conditions that explain in this section. These experiments were carried out to analyze the performance of this vehicle on typical sunny days. The DC voltage, DC current, vehicle speed torque, and load are the experimental parameters used to measure this vehicle's performance.

- *The Vehicle Maximum Speed with Load Variation:* The vehicle speed with load variation is illustrated in figure 8(a). These tests were conducted with the variable load ranging from no-load to 350 kg, which was the maximum weight the vehicle can hold. The maximum speed achieved at the different load conditions 0 kg, 70 kg, 140 kg, 210 kg, 280 kg, 350 kg were recorded 29 km/h, 27 km/h, 25 km/h, 23 km/h, 21 km/h, 19 km/h respectively. The maximum speed achieved at different load conditions directly depends on the pulling capability of the BLDC motor. The performance tests are carried out on a rectangular flat track for each load conditions.

- *The Torque Required with Load Variation at Different Speeds:* Torque is required to move the vehicle from a rest position. It is the essential factor used for acceleration of this vehicle but not used for maintaining speed. Figure 8(b) shows the torque required with load variation at different speeds. The value of torque needed is decreasing with increasing the speed of the vehicle for each load condition. The vehicle starts to move from a rest position, and it required higher initial torque. The vehicle travelled at speed less than 5 km/hr that need

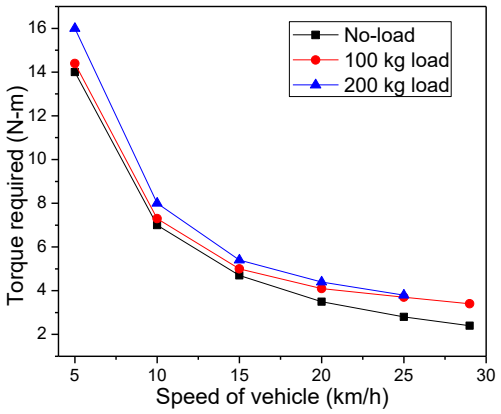

Fig. 8(b). The torque required with load variation at different speeds.

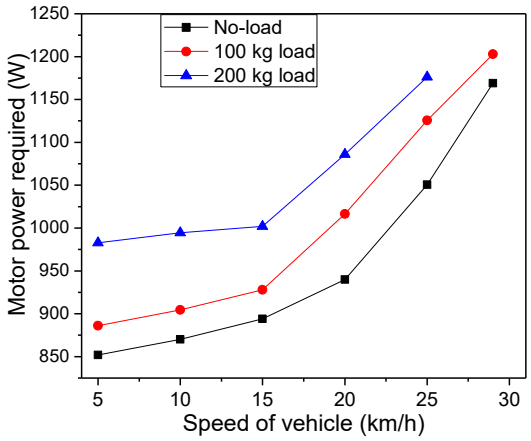

Fig. 8(c). The vehicle motor power consumption with load variation at different speeds.

14-16 N-m torque. At 25 km/hr speed, torque is reduced to the minimum value of 3-6 N-m. The vehicle was travelling with a speed less than 5 km/hr at that time it required 16 N-m maximum peak torque for 200 kg load condition.

- *The Vehicle Motor Power Consumption with Load Variation at Different Speeds:* Power consumption of motor is increased with increasing the speed of a vehicle for each load condition. Figure 8(C) shows the vehicle motor power consumption with load variation. The highest amount of motor power is consumed in loading conditions as compared to the no-load condition. The power consumed by the motor is varied between 850-1160 W at 200 kg load condition with increasing the speed of a vehicle, whereas for 100 kg load condition the power consumption varied between 886-1203 W. At no-load condition, the motor power consumption is recorded between the range 983-1176 W.
- *Covering effects of PV panels on the vehicle performance:* The solar panel covering affects this vehicle's performance, as shown in figure 8(d). The distance travelled by vehicle is decreased with

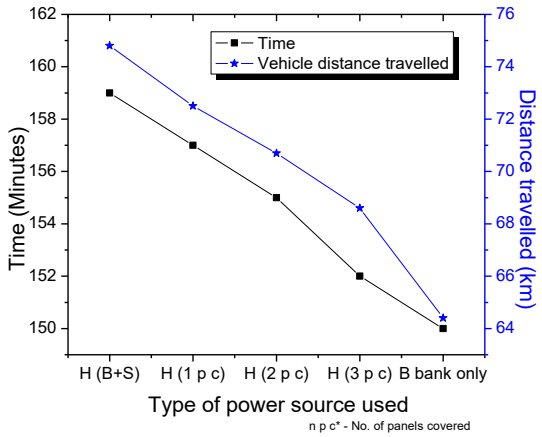

Fig. 8(d). Solar panel covering effects on vehicle performance.

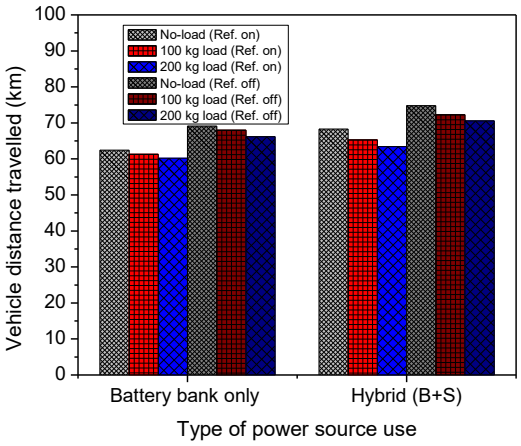

Fig. 8(e). Vehicle distance travelled at refrigerator on/off position.

increasing solar panel covering number. The vehicle was travelling a distance of 68.3 km in 159 minutes on hybrid energy (battery + solar on position) mode. The covering panel number was increased from 1 to 4; the vehicle was travelling 66.5 km, 64.7 km, 62.4 km, 64.4 km distance in 157 minutes, 155 minutes, 152 minutes, 150 minutes, respectively.

Vehicle Distance Travelled at Refrigerator On/Off position: The distance covered by the vehicle is depending on load-carrying capacity and type of power source use. The vehicle was travelling a higher distance in the hybrid mode of energy (Battey + solar) than the battery bank alone. The distance travelled by vehicle with the on and off position of a refrigerator is shown in figure 8(e).

The maximum 74.8 km distance covered by vehicle (no-load condition) is recorded in hybrid energy mode at refrigerator off position. The vehicle's total energy consumption was higher in hybrid energy mode for 200 kg load condition at the refrigerator on position, consuming 3450 Wh energy.

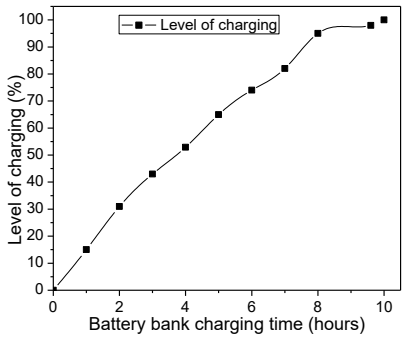

Fig. 8(f). Charging performance of battery bank.

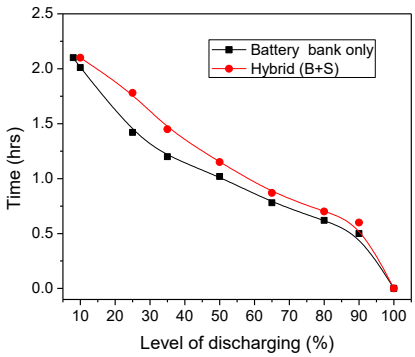

Fig. 8(g). Discharging performance of battery bank at 200 kg load condition.

- *Charging Performance of Battery Bank:* The grid electricity is the primary energy source used for charging the battery bank. The charging profile of the battery bank is shown in figure 8(f). The charging profile was linear up to 60%. However, after that rate of charging was slow, and the charging slope was decreasing. The battery bank required 8-9 kWh energy in 8-10 hr for full charging. The solar energy generated by solar panels was 2900-3600 Wh on an average sunny day. The time was requiring 18.9 hr for fully charging the battery bank with solar energy. Therefore, the vehicle was requiring 2.7 days for full charging with solar energy.
- *Discharging Performance of Battery Bank with and without Solar Energy:* The discharging profile of the vehicle at the refrigerator on a 200 kg load position is shown in figure 8(g). This vehicle's discharging performance is tested at the fridge on a 200 kg load position. The energy generates by PV panels in the daytime is support the battery bank. Therefore, the battery bank discharging rate is slow in hybrid energy mode. The battery bank's energy discharge rate is faster in battery mode than the hybrid energy mode for the same load condition.
- *Economic Analysis and Payback Period:* The economic analysis and the payback period are calculated based on the Indian E-vehicle market study.

Vehicle's total cost = A (cost of vehicle) + B (cost of refrigerating unit) + C (cost of solar unit)
Total cost= A (INR 140000.00) + B (INR 65000.00) + C (INR 26000.00) = INR 231000.00
Solar energy generates by vehicle solar unit = 2-4 kWh (depends on season)
Total solar energy generates by vehicle solar electricity unit per month = Avg. solar unit × 30 = 3.5 × 30 = 105 kWh
Average solar energy available in India 7-8 months per year
Average solar electricity unit generate per year = 105 × 8 = 840 kWh
Single unit cost in Punjab state = 6 INR
Average energy saved per year = 840 × 6 = 5040 INR
Average reservation of this vehicle in a single day = 2- 3 booking
One time booking cost of vehicle = 350-500 INR
Total average cash earn by vehicle in single day = Avg. booking in number × Avg. cost of booking = 2.5 × 425 =1062.5 INR
Cash earn by this vehicle per month = 1062.5 × 30 = 31875.00 INR
Cash earn by this vehicle per year = 31875 × 12 = 382500.00 INR
Total money earns by this vehicle per year = vehicle case earns per year + average energy saved per year = 382500 + 5040 = 387540 INR
Payback period of this vehicle = Total cost of refrigerated vehicle/Total money earns by this vehicle per year
Vehicle's payback period = 231000/387540 ≅ 6 months.

VI. CONCLUSION

The integral system of SAREV has been presented in this study. The performance analysis of this vehicle was tested with varying load conditions and study the effect on travelling distance. Experiments were conducted to evaluate the performance of the solar PV system, refrigeration system, and battery bank system, integral system, respectively. The integrated system was tested with different modes of energy and investigated the battery bank's charging and discharging performance. Based on the experimental results and the economic analysis, the significant findings obtained from this work are summarized as follows:

- The solar PV system was generating 2.96-3.6 kWh energy in the average sunny day.
- The vehicle's refrigerator was consuming 116 Wh energy in one day at thermostat position 7 to maintain -12 ^{o}C temperature inside the cabin.
- At the thermostat position 5, the refrigerator was maintaining the lower temperature (-10.6 ^{o}C) inside the cabin within minimum time (1hr) by consuming less energy (58 Wh).
- The maximum speed (29 km/h was recorded at no-load condition (self-weight of the vehicle).
- The speed of the vehicle was decreasing with increasing load on the vehicle. At 200 kg load condition, this vehicle was travelling at 23 km/h speed.

- The vehicle was travelling less than 5 km/hr speed that needed 14-16 N-m torque for each load condition. Torque was decreasing with the increasing speed of the vehicle. At 25 km/hr speed, torque reducing to the minimum value of 3-6 N-m for each load condition (0-200 kg).
- The motor power consumption was increasing with increasing the load and speed of the vehicle.
- The highest distance travelled by this vehicle was 74.8 km at refrigerator off condition by consuming 2970 Wh energy in hybrid energy mode.
- At the refrigerator on the condition, this vehicle's highest distance was 68.3 km by consuming 3010 Wh energy in hybrid energy mode.
- The vehicle travelling distance decreased 4-4.9 km/h at the refrigerator on position for each load condition.
- The energy consumption of the vehicle was increasing with the increasing load on the vehicle.
- This vehicle was required 8-10 hours and 8-9 kWh energy for fully charging the battery bank.
- The 17-21 hours in 3 days were required for fully charging the battery bank with solar energy.
- The discharging time of the battery bank was decreasing with increasing load on the vehicle. For the 200 kg load condition, the battery bank's discharging rate was lower in hybrid (S + B) energy mode.
- This vehicle has a smaller payback period (6 months) and the travelling cost of the vehicle was 1-1.5 INR per kilometer.
- The CO_2 emission by this vehicle was 13 gm/km lower than e-rikshaw and auto rikshaw (LPG, diesel, petrol).

ACKNOWLEDGMENT

This project was supported by the National Institute of Technology Jalandhar of India in TEQIP-II (R & D/1625).

REFERENCES

1. J. Benajes, A.García, J. Monsalve-Serrano, and S. Martínez-Boggio, "Emissions reduction from passenger cars with RCCI plug-in hybrid electric vehicle technology," Applied Thermal Engineering, vol. 164, pp. 114430, 2020.
2. M. Waseem, M. Suhaib, and A. F. Sherwani, "Modelling and analysis of gradient effect on the dynamic performance of three-wheeled vehicle system using Simscape," SN Applied Sciences, vol.1, no. 3, pp. 225, 2019.
3. D. Carlstedt and L. E. Asp, "Performance analysis framework for structural battery composites in electric vehicles," Composites Part B: Engineering, vol. 186, pp. 107822, 2020.
4. V. Prabhu, S. K. Gupta, S. Madhwal, and V. Shridhar, "Exposure to atmospheric particulates and associated respirable deposition dose to street vendors at the residential and commercial sites in Dehradun City," Safety and health at work, vol. 10, no. 2, pp. 237-244, 2019.
5. F. Calise, F. L. Cappiello, A. Cartenì, M. D. d'Accadia, and M. Vicidomini, "A novel paradigm for a sustainable mobility based on electric vehicles, photovoltaic panels and electric energy storage systems: Case studies for Naples and Salerno (Italy)," Renewable and Sustainable Energy Reviews, vol. 111, pp. 97-114, 2019.
6. P. Ahmadi, "Environmental impacts and behavioural drivers of deep decarbonization for transportation through electric vehicles," Journal of Cleaner Production, vol. 225, pp. 1209-1219, 2019.
7. R. M. Prasad, and A. Krishnamoorthy, "Design, construction, testing and performance of split power solar source using mirror photovoltaic glass for electric vehicles," Energy, vol. 145, pp. 374-387, 2018.
8. W. Pang, H. Yu, Y. Zhang, and H. Yan, "Solar photovoltaic based air-cooling system for vehicles," Renewable energy, vol. 130, pp. 25-31, 2019.
9. S. Angadi, D. C. Badiger, U. K. R. Yaragatti, and A. B. Raju, "Experimental verification of MPPT algorithms for photovoltaic systems," International Journal of Recent Technology and Engineering, vol. 8, pp. 124-129, 2020.
10. https://www.worldweatheronline.com/jalandhar-weather-averages/punjab/in.aspx. Accessed on 20.09.2020.
11. C. Lodi, A. Seitsonen, E. Paffumi, M. De Gennaro, T. Huld, and S. Malfettani, "Reducing CO_2 emissions of conventional fuel cars by vehicle photovoltaic roofs," Transportation Research Part D: Transport and Environment, vol. 59, pp. 313-324, 2018.
12. G. Li, "Comprehensive investigation of transport refrigeration life cycle climate performance," Sustainable Energy Technologies and Assessments, vol. 21, pp. 33-49, 2017.
13. B. B. Gardas, R. D. Raut, and B. Narkhede, "Modeling causal factors of post-harvesting losses in vegetable and fruit supply chain: an Indian perspective," Renewable and sustainable energy reviews, vol. 80, pp.1355-1371, 2017.
14. https://ourworldindata.org/search?q=electric+vehicle. Accessed on 25.09.2020.
15. S. Kumar, and R. S. Bharj, "Solar hybrid e-cargo rickshaw for urban transportation demand in India," Transportation Research Procedia, vol. 48, pp. 1998-2005, 2020.
16. C. P. Darji, "IoT based sensor for humidity and temperature measurement in smart HVAC systems," International Journal of Recent Technology and Engineering, vol. 9, pp. 42-44, 2021.
17. S. A. Tassou, G. D. Lille, and Y. T. Ge, "Food transport refrigeration–Approaches to reduce energy consumption and environmental impacts of road transport," Applied Thermal Engineering, vol. 29, pp. 1467-1477, 2009.
18. B. Li, R. Otten, V. Chandan, W. F. Mohs, J. Berge, and A. G. Alleyne, "Optimal on-off control of refrigerated transport systems," Control Engineering Practice, vol. 18, pp. 1406-1417, 2010.
19. P. Glouannec, B. Michel, G. Delamarre, and Y. Grohens, "Experimental and numerical study of heat transfer across the insulation wall of a refrigerated integral panel van," Applied Thermal Engineering, vol. 73, pp. 196-204, 2014.
20. T. L. Micheaux, M. Ducoulombier, J. Moureh, V. Sartre, and J. Bonjour, "Experimental and numerical investigation of the infiltration heat load during the opening of a refrigerated truck body," International Journal of Refrigeration, vol. 54, pp. 170-189, 2015.
21. A. Rai and S. A. Tassou, "Environmental impacts of vapor compression and cryogenic transport refrigeration technologies for temperature-controlled food distribution," Energy Conversion and Management, vol. 150, pp. 914-923, 2017.
22. B. Michel, P. Glouannec, A. Fuentes, and P. Chauvelon, "Experimental and numerical study of insulation walls containing a composite layer of PU-PCM and dedicated to the refrigerated vehicle," Applied Thermal Engineering, vol. 116, pp. 382–391, 2017.
23. A. Meneghetti, G.D. Rold, and G. Cortella, "Sustainable refrigerated food transport: searching for energy-efficient routes," IFAC, vol. 51, pp. 618-623, 2018.
24. P. Artuso, A. Rossetti, S. Minetto, S. Marinetti, L. Moro, and D. D. Col, "Dynamic modelling and thermal performance analysis of a refrigerated truck body during operation," International Journal of Refrigeration, vol. 99, pp. 288-299, 2019.
25. P. B. Jara, J. J. Rivera, C. E. Merino, E. V. Silva, and G. A. Farfan, "Thermal performance of a refrigerated vehicle: Process simulation," International Journal of Refrigeration, vol. 100, pp. 124-130, 2019.
26. M. Merai, D. Flick, L. Guillier, S. Duret, and O. Laguerre, "Experimental characterization of heat transfer inside a refrigerated trailer loaded with carcasses," International Journal of Refrigeration, vol. 99, pp. 194-203, 2019.
27. F. Wang, M. Li, Y. Zhang, X. Liu, D. Xie, Q. Zhang, and H.Yang, "Study on roof-mounted radiant cooling system for LNG-fueled refrigerated vehicles," International Journal of Low-Carbon Technologies, pp. 1-7, 2020.
28. C. Kurien, A. K. Srivastava, and E. Molere, "Indirect carbon emissions and energy consumption model for electric vehicles: Indian scenario," Integrated Environmental Assessment and Management, vol. 16, no. 6, pp. 998-1007, 2020.
29. P. V. Brockdorff and G. Tanti, "Carbon emissions of plug-in electric vehicles in Malta: A policy review," Case Studies on Transport Policy, vol. 5, no. 3, pp.509-517, 2017.

30. V. B. Raju and C. Chengaiah, “A novel T-C-T solar photovoltaic array configurations using rearrangement of PV modules with shade dispersion technique for enhancing the array power,” International Journal of Recent Technology and Engineering, vol. 8, pp. 68-78, 2020.